

# Effect of Phase Transformation and Tin Addition on the Creep Characteristics of Al-Ag Alloy

R. H. Nada<sup>a</sup> and H. Y. Zahran<sup>a,b</sup>

a) Department of Physics, Faculty of Education, Ain Shams University, Cairo, Egypt

b) Department of Physics, Faculty of Science, King Khalid University, Abha, KSA

**Abstract**— Wire samples of both Al- 2wt% Ag and Al- 2wt% Ag- 1wt% Sn alloys were prepared by normal casting technique from highly pure elements. Creep measurements were carried out under the applied stresses, 116.77, 119.27 and 121.76 MPa, for samples aged for 2 hours in the temperature range, 513- 563 K. Increasing the applied stress and/or the aging temperature and irregular order in the creep curves at 543K were showed itself as a drop in the measured values of the creep parameters. The stress sensitivity parameter,  $m$  and the activation volume,  $V$ , at the transformation temperature, 543K, which is above all of them increased again. All the obtained data show that the ternary alloy, containing Sn, is softer than the binary alloy. Sn addition improved the tensile ductility of the alloy under the testing conditions. The activation energy values (in  $\text{kJ}\cdot\text{mol}^{-1}$ ) before and after transition were measured. The microstructure of the samples was obtained by transmission electron microscopy (TEM).

**Index Terms**— Creep; Steady state stage; Phase transformation; Activation energy; Activation volume; microstructure; tensile ductility.

## 1 INTRODUCTION

The Al-Ag based alloys are often used in technological applications because of their easy casting and coarsening of plate-shaped precipitates. Also this system serves as a useful model for better understanding of the kinetics of the precipitation and the coarsening of plate-shaped precipitates [1]. Silver has a strong tendency to bind quenched in vacancies which leads to faster formation of intermediate clusters. This promotes nucleation of phases during aging supersaturated quenched silver containing alloy [2]. Al-Ag based alloys are more desirable because of their higher strength and excellent thermal stability, but they are more expensive and difficult to creep-form [3]. Improvement and optimizing the mechanical properties have been achieved by the addition of alloying elements to binary alloys [4]. Al-Ag samples quenched from a high temperature in the solid solution field to room temperature that makes the solid solution supersaturated with the vacancies and solute atoms. This tends to precipitate in some form or another causing increased hardness [5].

Al-Ag alloys are very low interfacial energies, so that, it was reported by Legoues and Wright [6] that homogeneous nucleation of G.P. zones is so easy, that it begins almost as soon as the solvus line is crossed during quenching from the solution annealing treatment, before the spinodal region is reached.

The equiaxed G.P. zones in the aged supersaturated Al-Ag alloys precipitate because of the small difference of atomic radii (0.5%) between the solvent Al and the solute Ag atoms. The formation of G.P. zones was attributed [7] to the existence of a meta-stable miscibility gap. Two states of G.P. zones were suggested to exist before the  $\gamma$  and  $\beta$  precipitates evolve: (i)  $\eta$ -state of presumably ordered precipitates and homogene-

ous in composition with a critical temperature of 500 K, and composition of 55-60 at % Ag, (ii) internally inhomogeneous  $\eta$ -state of Ag-segregated clusters with critical temperature of 720 K and composition of 30 at % Ag. The sudden change in composition of the zones around 443 K was caused by the transformation from the low temperature,  $\eta$ -state (below 443 K) to the high temperature  $\epsilon$ -state (above 443 K)[8]. Reversion of some G.P. zones during aging above 443 K into  $\gamma$ -plates has been reported by Shchegoleva and Meteloved [9].

It was indicated that the crystalline structures of  $\eta$  - state (low temperature) and  $\epsilon$  - state (high temperature), G.P. zone precipitates should be long- range ordered and disordered, respectively[10]. Even though the atomic radii of Al and Ag atoms differ by only 0.5%, there still exists a strain field surrounding G.P. zones. These new information was reported although their contrast, the ordered state for the  $\mu$  zones was disproved [11]. Different models were presented for  $\epsilon$ - zones to be either of the silver- depleted shell or the silver- depleted core, which was confirmed [12].

It is aimed to investigate the effect of 1wt% Sn addition on the aging behaviour and the creep characteristics of the binary Al-2wt%Ag alloy. Transmission electron microscopy (TEM) was used to trace the thermally induced changes in the microstructure and the mechanical properties under the same different aging conditions.

IJSER staff will edit and complete the final formatting of your paper.

## 2 EXPERIMENTAL PROCEDURE

The tested alloys Al-2 wt.% Ag (alloy B), and Al-2 wt.% Ag - 1wt.% Sn (alloy T) were prepared under the same conditions, from Al, Ag and Sn elements of purity 99.99%, by melting each alloy content in a graphite crucible together with calcium chloride  $\text{CaCl}_2$  flux to prevent oxidation. The rod shape ingots

• Author name: Radwan H. Nada - PhD. In Ain Shams University, Cairo, PH-0020238116435. E-mail: radwanhnada@yahoo.com

were homogenized at 773K for 3 days, then swaged into wires of 0.5 mm diameter for creep study, and sheets of 2 mm thick for electron microscopy investigation. The samples were annealed for 2 h at 806 K, and then quenched in iced water to obtain the supersaturated  $\alpha$ -solid solution structure. The samples were aged for 2 hours in the temperature range, 513-563K, in steps of 10 K. A conventional - type tensile testing machine is described elsewhere [13], which was employed to obtain the creep measurements at room temperature under the stresses, 116.77-119.27 and 121.76 MPa. The sheet specimens for electron microscopy investigation were prepared by electro-polishing using a twin jet machine. The used solution was 25% nitric acid and 75% ethanol at 273 K. The voltage and current values were around 4 V and 90 mA. Microstructures were examined using a JOEL JM-100 transmission electron microscope operating at 100 kV.

**3 Experimental results**

The creep curves for both alloys (Al- 2wt%Ag) and (Al-2wt%Ag- 1wt%Sn) showing the same normal creep behaviour. The transient creep strain  $\epsilon_{tr}$  which is characterized by a decreasing strain rate is given [14] as;

$$\epsilon_{tr} = \beta t^n, \tag{1}$$

where the transient creep time (t), the time exponent (n) and the creep constant ( $\beta$ ) are the transient creep parameters which depend on both the temperature and the applied stress. Fig. 1 shows that, the parameters  $\beta$ , and n, increases with increasing of temperature and/or applied stress.

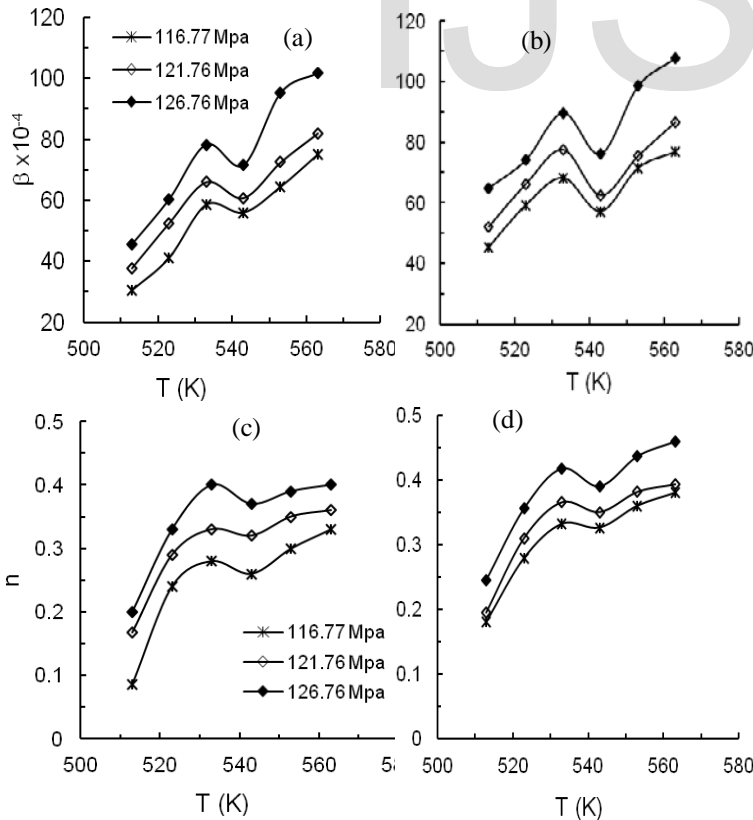


Fig. 1- The temperature dependence of the transient creep parameters:  $\beta$ , (a, b) and n, (c, d) for both alloys B and T.

The transient creep parameter  $\beta$  changes [15] when the aging temperature, T, change according the following Arrhenius-type relation:

$$\beta = \text{const. exp} (-Q/KT) \tag{2}$$

where Q is the activation energy (in kJ/mol) and K is Boltzmann constant. The activation energies before and after transformation were calculated for the transient stage from the slopes of the temperature dependent straight lines which were the relation between  $\ln \beta$  and  $(1000/T) K^{-1}$ , as in Fig. 2. The steady state creep rate  $\dot{\epsilon}_{st}$ , was obtained from the creep curves, as shown in Fig. 3, which increased by increasing the aging temperature.

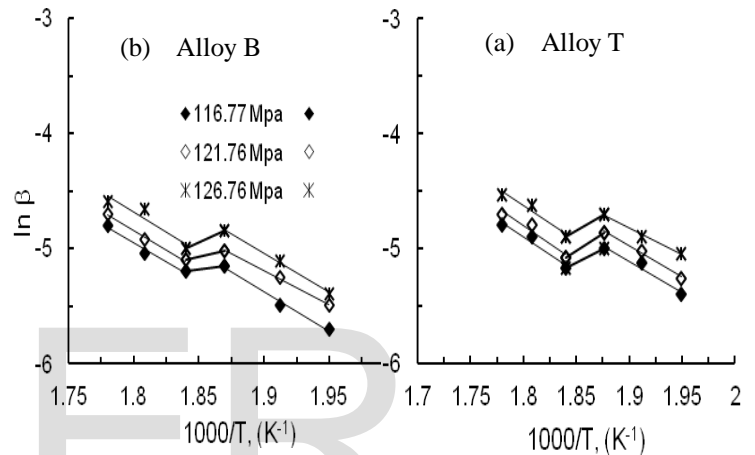


Fig.2- The relation between  $\ln \beta$  and  $(1000/T) K^{-1}$ , for the transient stage.

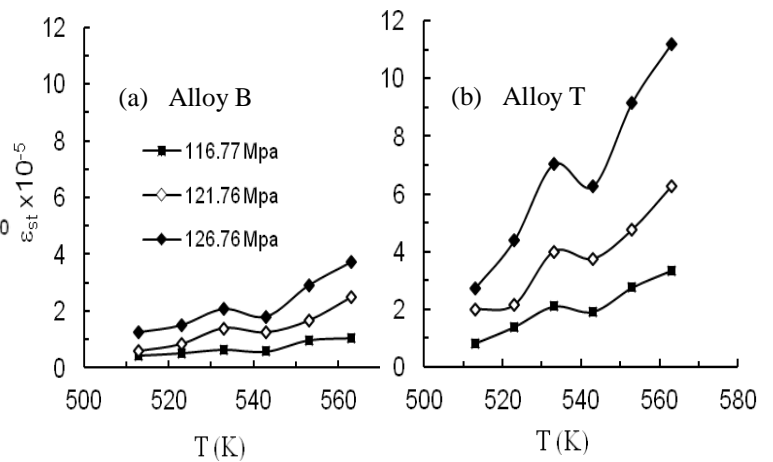


Fig. 3- The aging temperature dependence of the steady state creep rate  $\dot{\epsilon}_{st}$ .

The activation energies, for the steady state stage, before and after transformation were calculated from the slopes of the temperature dependent straight lines relating  $\ln \dot{\epsilon}_{st}$  and  $(1000/T) K^{-1}$ , shown in Fig. 4.

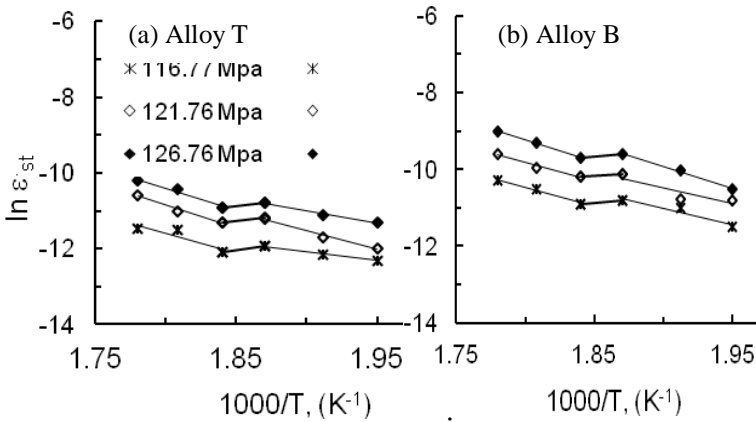


Fig. 4- The relation between  $\ln \dot{\epsilon}_{st}$  and  $(1000/T) K^{-1}$  for the steady state stage.

The values of the stress sensitivity parameter,  $m = \ln \dot{\epsilon}_{st} / \ln \sigma$ , have been calculated from the slopes of the straight lines, as in Fig.5a, while the activation volume  $V = \ln \dot{\epsilon}_{st} / \sigma$  is result from the slopes of the straight as in Fig. 5b. The behaviour of the aging temperature dependence of the stress sensitivity parameter,  $m$ , and the activation  $V$ , given in Fig.6 and Fig. 7, respectively for both alloys, is similar to the behaviour of  $\beta$  and  $n$ , in Fig.1b, and  $\dot{\epsilon}_{st}$ , Fig. 3. All these parameters, increased by increasing aging temperature. We noticed a drop at 543 K followed by the continuous increase above 543K, establishing the two relaxation stages around the transformation temperature 543K.

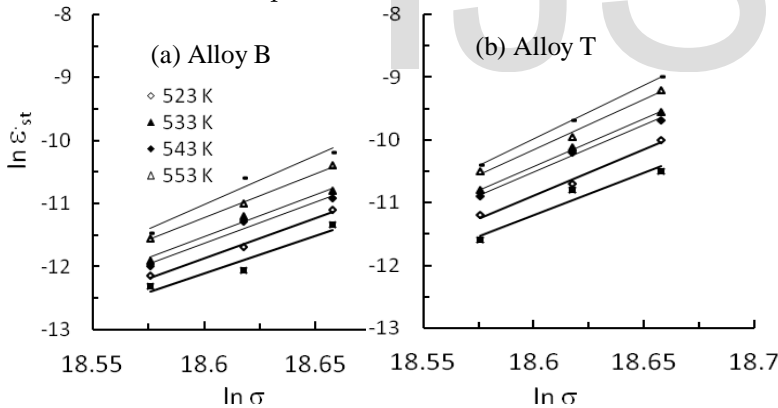


Fig. 5- The relation between  $\ln \dot{\epsilon}_{st}$ , and  $\ln \sigma$  at different aging temperatures.

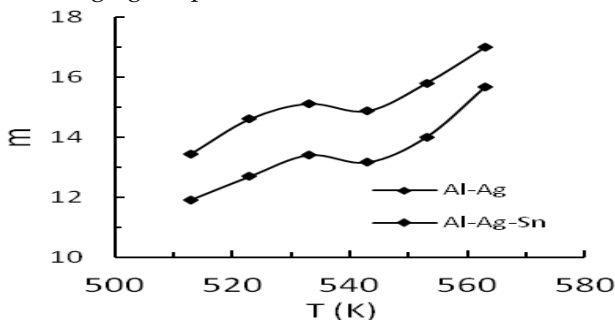


Fig.6- The aging temperature dependence of the stress sensitivity parameter,  $m$ .

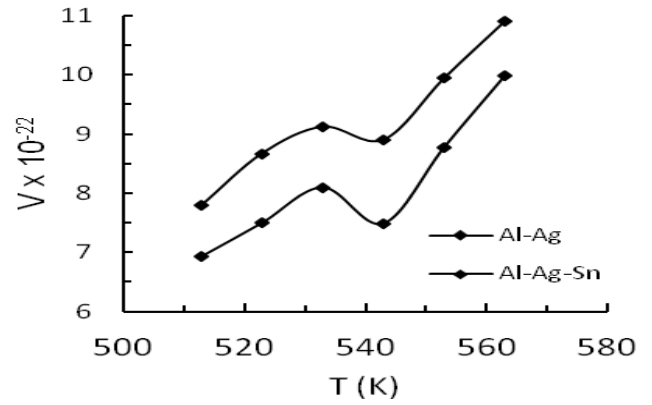


Fig. 7- The aging temperature dependence of the activation volume  $V$ .

The micro-graphs of Fig. 8 were obtained for sheet samples of both alloys homogenized, solution treated, quenched and aged at (533, 543, and 553 K).

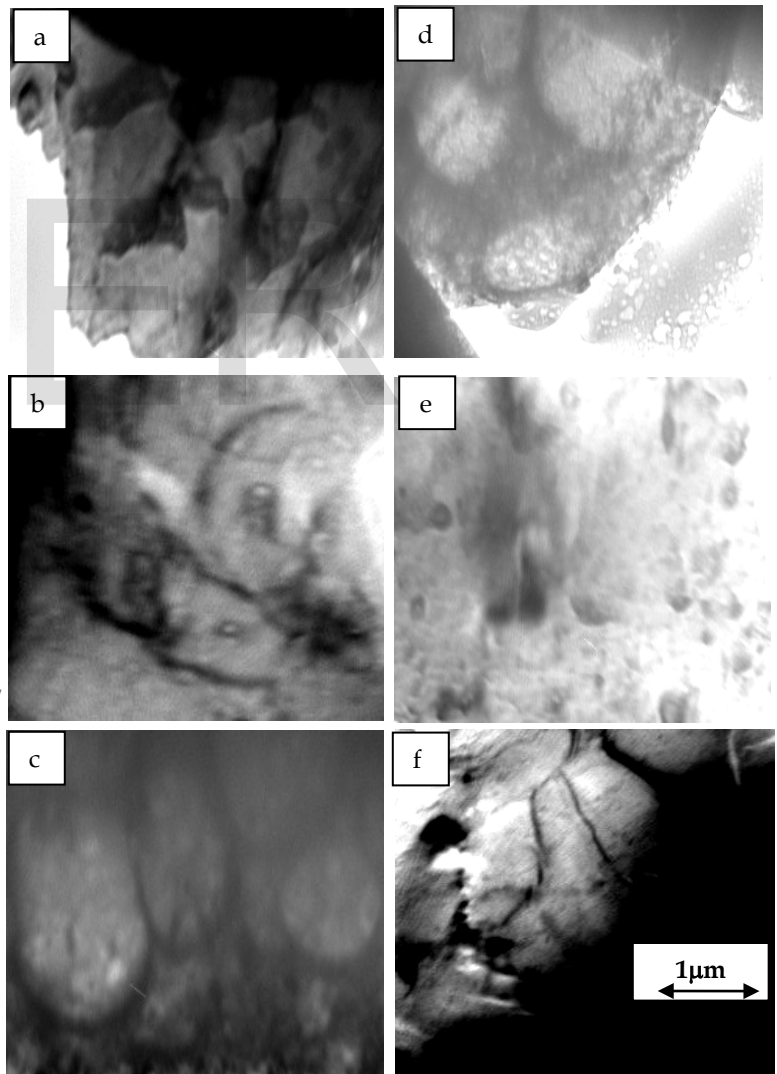


Fig. 8- Room temperature micro-graphs obtained for sheets of: alloy B (a, b, c) and alloy T (d, e, f), aged at (533, 543, and 553K).

## 4 DISCUSSION

Al-Ag samples quenched from a high temperature in the solid solution field to room temperature that makes the solid solution supersaturated with the vacancies and solute atoms. This tends to precipitate in some form or another causing increased the hardness. The changes in the physical properties during aging, may be either due to the solid solution passing through a state of pre-precipitation characterized by a different atomic structure, or that the alloy contains precipitates so fine that they escape observation.

In the micrographs of Fig. 8, the white phases are the matrix  $\alpha$  (Al) where most of them belong to dendrite crystal. The black phases are inhomogeneous structure of Ag fine, coarse particles of  $\epsilon$ -state GP zones and meta-stable  $\gamma$  phase. Both of GP zones and  $\gamma$  phase form thick boundaries for the enveloped dendrite crystals of  $\alpha$  (Al matrix). The gray reticulate phases are the Sn phases in the ternary alloy disperse in the  $\alpha$  (Al matrix) and the Ag-depleted cores. This may stabilize some Sn and Ag particles and consequently lower their hardening effect. Moreover, Sn prevents the formation of the high strength large plate-like structure which forms in the binary alloy. This makes the samples of the ternary alloy T, softer than the samples of the binary Al-Ag alloy.

The primary and steady state creep stages in Al-Ag alloys containing regions of G.P zones or  $\gamma$ - plates that may be the result of combined action of a hardening and recovery processes, that force created dislocations to move through the matrix under the creep recovery mechanisms, depending on the interaction between these precipitates and dislocations. Above transition temperature, the dislocation motion in G.P. zones [16] region is slower than that in the solid solution region. This is consistent with the higher values of  $n$ ,  $\beta$  and  $\dot{\epsilon}_{st}$  in Figs. (1 and 3), the stress sensitivity parameter  $m$ , Fig. 6, and the activation volume  $V$ , Fig. 7, above the transition temperature 543K compared with those in the G.P. zones region.

In general, the increase of  $n$ ,  $\beta$ ,  $\dot{\epsilon}_{st}$ ,  $m$  and  $V$  values by increasing aging temperatures, Figs. (1, 3, 6 and 7) respectively, occur due to raising the temperature that makes easier dislocations overcome obstacles in the matrix. This due to the annihilation or clustering of large amounts of the quenched-in vacancies which reduces the density of dislocation pinning points; or, the increase of temperature which leads to gradual recovery of internal strains until reaching to the hardness level caused by the presence of the second phase atoms in the matrix[4].

Below 543 K,  $m$  and  $V$ , increases with increasing of temperature, this is due to some ordering in the dislocations and the defect systems affected by the thermal agitation which makes easier the motion of dislocations and lower values of  $m$  and  $V$  are expected at such temperatures [17].

Up to the transition temperature, 543 K, the increase of  $n$ ,  $\beta$ ,  $\dot{\epsilon}_{st}$ ,  $m$  and  $V$ , values are attributed to the amount of the second phase existing and its corresponding diffusivity with the matrix which control the dislocation mobility at the inter-

face boundary[18]. Aging the solution treated samples, the precipitated  $\alpha$  (Al) and  $\beta$  (Ag)-phases coarsen and the solubility of Ag in Al increases by increasing temperature leading to the formation of widely separated less number of large precipitated particles which increase the values of  $m$ ,  $V$  and reduce the strength in this stage, as shown in Fig. 6, Fig. 7, Fig. 8a, at 533 K and Fig. 8b, at 543 K. In this temperature range at 493K [19], or 498K [20], the start of small size coherent  $\gamma$ - precipitates formation takes place. At 543K the formation of an important quantity of  $\gamma$ -precipitate particles and the increased area of the coherent  $\gamma$ - matrix interfaces provides a major barrier to dislocation motion and increases the strength of the alloy leading to the observed drop in the measured values of all parameters. This agrees with the maximum Vickers hardness which were reported before [19] when the volume fraction of continuous precipitation was higher, Fig.8.

Above the transition temperature, the precipitated ( $\alpha + \beta$ )-phases transform into f.c.c.  $\alpha$ -solid solution phase, so the  $\beta$ -phase dissolves completely and disappears (as shown in Fig. 8c, at 553K) to attain the equilibrium composition [21].

The higher values of the parameters obtained at higher temperatures are attributed to the reduced crack initiation life associating the existing large grain size. In this stage, above 543 K, the rapid increase of  $n$ ,  $\beta$  and  $\dot{\epsilon}_{st}$  values are due to the subsequent coalescence and partial dissolution of G.P zones and the early stages of precipitation of coherent meta-stable  $\gamma'$ - phase achieved on the expense of the number of G.P zones (as shown Fig. 8c). Both coarse G.P zones of small numbers and smaller-sized  $\gamma'$ -precipitates with a relatively lower density provide small barriers to dislocation motion resulting in a relatively lower strength [20]. Values of  $m$ , in Fig. 6, show that the dominating mechanism in the low temperature region (below 543 K) is dislocation glide, while in the high temperature region the dominating mechanism is dislocation climb [22].

The activation energy values (in kJ/mol) before and after transition were 48, 57.6 in alloy B, and 51, 60 in alloy T, for the transient creep stage while 72.96, 96 for alloy B, and 90.53, 105.6, for alloy T in the steady creep stage. Thus, it is reasonable to correlate the values obtained for the activation energy with the sequences of the precipitation processes that take place in the matrix during deformation controlled by just a grain boundary diffusion mechanism [23], before transformation temperature (543 K) and a dislocation glide mechanisms after transformation [24].

Although alloying the Al-Ag alloy, (Alloy B), with Sn is expected to harden it [4], the observations in the present data show continuous softening and improved tensile ductility behaviour for the samples of the alloy T containing Sn under the same testing conditions for alloy B. This can be explained as follows.

It may be that the difference in ductility between the Ag precipitate particles, (Young's modulus  $Y_{Ag} = 80.5 \text{ GNm}^{-2}$ ), which

are harder, than the Al matrix, ( $Y_{Al} = 71 \text{ GNm}^{-2}$ ), and the added Sn ( $Y_{Sn} = 52 \text{ GNm}^{-2}$ ), makes the whole structure similar to a non-Newtonian fluid containing rigid particles [25] which rotate practically without deformation while the soft Sn-phase undergo plastic deformation performing accommodation between both by sliding along the interfaces [26].

## 5 CONCLUSION

The increase of the creep parameters  $n$ ,  $\beta$ ,  $\dot{\epsilon}_{st}$ ,  $m$ , and  $V$ , for both alloys B and T, with increasing aging temperature and/or the applied stress, was interrupted by a drop at the transformation temperature, 543K, above which it raised again to higher levels than those before transformation.

Adding Sn prevents the formation of high strength large plate-like structure which formed in the binary alloy. Therefore, the expected role of Sn as a hardening alloying element changed, making the samples of the ternary alloy T, softer than the samples of the binary alloy B.

The obtained activation energies suggest the grain boundary diffusion and the dislocation glide mechanisms to control the creep process.

## 6 References

- [1] M.A. Mahmoud, G. Graiss, J. Mater. Sci. 37 (2002) 2215- 2221.
- [2] D.Vakavos, P.B.Prangnell, B. Bes, F.Eberl; Mater. Sci. Eng. A 491 (2008) 214- 220.
- [3] R.N. Lumley, I.J. Polmear, Scr. Mater. 50, (2004) 1227- 1232.
- [4] F. Abd El-Salam, A. M. Abd El-Khalek, R.H. Nada, L. A. Wahab, H.Y. Zahran, Mater. Sci. Eng. A 527 (2009) 281-287.
- [5] G. Thomas, Philos. Mag. 4, 606 (1959) 1213- 1218.
- [6] F.K.Legoues, R.N.Wright, Y.W.Lee, H.I. Aaronson, Acta Metall. 32 (1984) 1865-1870.
- [7] G. Borelius, L.E. Larson, Ark. Fys. 11 (1956) 137-142.
- [8] T. Kanadia, A. Umada, Phys. Stat. Sol. A 148 (1995) 23-27.
- [9] T.V. Shchegoleva, Fiz. Met. Metalloved, 55 (1983) 59- 65.
- [10] M. Asta, D.D. Johnson, Comput. Mater. Sci. 6 (1997) 64- 69.
- [11] J.E.Gragg, J.B. Cohen, Acta Metall. 119 (1971) 507- 512.
- [12] Changrong Li, Chunju Niu, Zeting Du, Cuiping Guo, Yongjuan Jing, CALPHAD: Computer Coupling of Phase Diagrams and Thermochemistry 34 (2010) 120.
- [13] F. Abd El-Salam, R.H. Nada, A.M. Abd El-Khalek, Physica B 292 (2000) 71- 76.
- [14] F.Abd El-Salam, A.M. Abd El-Khalek, R. H. Nada; Physica B 388 (2007) 219- 224.
- [15] F.Abd El-Salam, A.M.Abd El-Khalek, R.H.Nada; Eur. Phys. J.AP 12 (2000) 159- 163.
- [16] Hossein OLIA, Mehrdad ABBASI, Seyed Hossein RAZAVI; Trans. Nonferrous Met. Soc. China 22 (2012) 312- 317.
- [17] G.S. Al-Ganainya, A. Fawzy, F. Abd El-Salam, Physica B 344 (2004) 443- 447.
- [18] R. Abd-El Hasseb, M.Sc. Degree. Physics department, Faculty of education, Ain shams university, Cairo, Egypt, (1996).
- [19] D. Hamana, Z. Boumerzoug, M. Fatmi, S. Chekroud, Materials chemistry and Physics 53 (1998) 208- 213.
- [20] M.A. Mahmoud, Physica. B 304 (2001) 456- 460.
- [21] M. Hansen, Constitution of Binary Alloys, McGraw-Hill Publishing Co, New York, 1100 (1958).
- [22] M. M. Mostafa, Journal of Physics 50, 9 (2000) 1051- 1055.
- [23] G.H. Deaf, S.B. Youssef, M.A. Mhmoud, Phys. Stat. Sol. A 168 (1998) 389- 394.
- [24] O. Ozawa and H. Kimura, Mater. Sci. Eng. 8 (1971) 327- 331.
- [25] M. Suery, B. B. Baudalet, Phil. Mag.; 41 (1980) 41- 45.
- [26] E.H. Toscano, Scr. Metall; 17 (1983) 309- 314.